

A Methodology for Approximating BPSK Demodulator Performance in the Presence of Various Undesired Signals

Michael Cotton

Institute for Telecommunications Sciences

Boulder, Colorado 80305

Email: mcotton@its.blrdoc.gov

This paper describes a methodology for analyzing binary phase-shift keyed demodulator performance in the presence of various types of undesired signals. It utilizes models of the underlying random processes to determine the probability of a bit error. The basic calculation involves integrating the probability distribution function of the internal receiver noise (assumed to be Gaussian) plus the undesired signal. When this integral cannot be solved analytically, a sample-function analysis is utilized. Results are given that compare the effects of various undesired signals (i.e., continuous-wave, MPSK, impulsive noise, and gated noise) to those of Gaussian noise.

1. INTRODUCTION

This paper describes a methodology for the statistical analyses of various undesired signals plus receiver noise to determine how the signals affect demodulator performance. The work is funded jointly by the Office of Spectrum Management (NTIA/OSM) as part of *The President's Spectrum Policy Initiative* [1] and the Institute for Telecommunication Sciences (NTIA/ITS). NTIA/OSM will use the methodology to evaluate the interference effects of new spectrum sharing technologies. NTIA/ITS will use it to validate interference susceptibility measurements and support generalized receiver research.

2. METHODOLOGY

This analysis focuses on the detector subsystem of a binary phase-shift keyed (BPSK) digital receiver, which is responsible for transforming the complex baseband (CBB) received signal into information bits. Ideal BPSK receiver operation is assumed, so that the uncorrupted received source signal produces $\pm A$ when sampled, and all deleterious effects are caused by the undesired signal plus receiver noise. Amplification and down-conversion prior to demodulation are assumed to cause negligible effects beyond their intended functions. Within the demodulator, the receiver filter is a matched root-raised cosine (RRC) filter and the sampler is optimally synchronized. The RRC filter is specified by its roll-off factor (a) and cutoff frequency (f_0). For our purposes, RRC parameters are chosen as $a = 0.35$ and $f_0 = 0.5$ MHz. An important trait of the RRC filter is that the noise equivalent bandwidth $b = 2f_0 = T^{-1}$, where T is the bit period. Lastly, a typical operational scenario is specified by setting the signal-to-noise ratio (P_s/P_n) to approximately 8.4 dB; this corresponds to a probability of a bit error (\mathcal{P}_e) due to receiver noise of 10^{-4} .

\mathcal{P}_e is calculated from first-order statistics of the undesired signal plus receiver noise. For simple undesired signals, analytic solutions are available. Beyond the simple cases, a combination of analytic and simulation methods are used to approximate \mathcal{P}_e . In this quasi-analytic approach, a sample function of the undesired signal plus receiver noise is simulated and bandlimited by the receiver filter. \mathcal{P}_e is approximated as the number of samples that cause an error divided by the total number of samples in the sample function.

The undesired CBB signals considered here are:

- Complex Gaussian noise (CGN)
- Constant signal
- M-ary phase-shift keyed (MPSK) signal
- Impulsive noise
- Gated noise

CGN is a baseline to which the other undesired signals are compared. It also emulates the noisy nature of many modern ultrawideband (UWB) devices. A constant signal emulates an interfering spectral line due to a continuous-wave (CW) signal or a signal that is periodic in nature. MPSK is representative of co-channel interference-limited scenarios, while impulsive noise is representative of man-made noise limited scenarios. Gated noise emulates UWB signals that periodically turn on and off or hop in and out of the operational frequency band of the victim receiver.

Recent research [2] has explored the relationship between \mathcal{P}_e and the amplitude probability distribution (APD), which characterizes first-order amplitude statistics. At this point, this topic has not been fully evaluated for the undesired signals considered in this work. However, in support of this research, APDs have been provided along with the corresponding \mathcal{P}_e plots.

3. THEORETICAL ANALYSES

Analytic solutions for \mathcal{P}_e are available for undesired signals plus receiver noise (at the output of the victim receiver filter) that can be described accurately with a statistical model. This is the case for three BPSK operational environments: (1) receiver CGN in the absence of undesired signals, (2) undesired CGN + receiver CGN, and (3) undesired constant + receiver CGN.

Figure 1 illustrates signals and relevant reference points within the victim receiver. At the output of the receiver filter, $\hat{r}(t) = \hat{s}(t) + \hat{v}(t)$ is the received signal and $\hat{s}(t)$ is the received source signal uncorrupted by receiver noise and undesired signals. The composite undesired-plus-noise signal is given by

$$\hat{v}(t) = [\hat{u}(t) + \hat{\xi}(t)] * \hat{h}_R(t) = \hat{u}(t) * \hat{h}_R(t) + \hat{n}(t) \quad (1)$$

where $\hat{u}(t) + \hat{\xi}(t)$ is the undesired-plus-noise signal before the receiver filter, $\hat{h}_R(t)$ is the impulse response of the receiver filter, $\hat{n}(t)$ is the receiver CGN after the receiver filter, $\hat{\cdot}$ denotes CBB, and $*$ is the convolution operator.

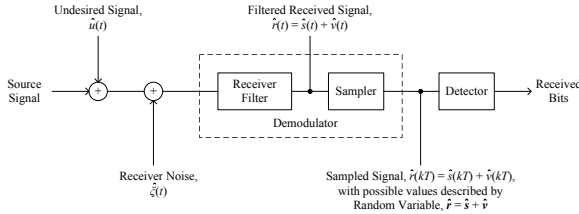


Fig. 1: Block diagram of the demodulator and detector subsystems inside a BPSK receiver with relevant signal nomenclature.

It is assumed that $\hat{r}(t)$ is optimally sampled at time kT within the k^{th} bit period, so that the sampled source signal, $\hat{s}(kT)$, is either $\mp A$ depending on whether a binary 0 or 1 was sent, respectively. Performance results are based on the detector decision process of the victim receiver. BPSK bit error probability is based on the real part of the sampled signal, i.e.,

$$r_x(kT) = \text{Re}[\hat{s}(kT) + \hat{v}(kT)] \quad (2)$$

where subscript x denotes the real part. The detector is a threshold device that decides a binary 0 was sent if $r_x(kT) \leq 0$ and a binary 1 was sent if $r_x(kT) > 0$. As illustrated in Figure 2(a), errors occur in two ways: (1) if $r_x(kT) > 0$ when a binary 0 was sent, and (2) if $r_x(kT) \leq 0$ when a binary 1 was sent.

In this study we are only interested in first-order statistics, hence, the discrete random processes $r_x(kT)$, $\hat{s}(kT)$, and $\hat{v}(kT)$ can be represented with random variables (RVs) \mathbf{r}_x , $\hat{\mathbf{s}}$, and $\hat{\mathbf{v}}$, respectively. Note that bold

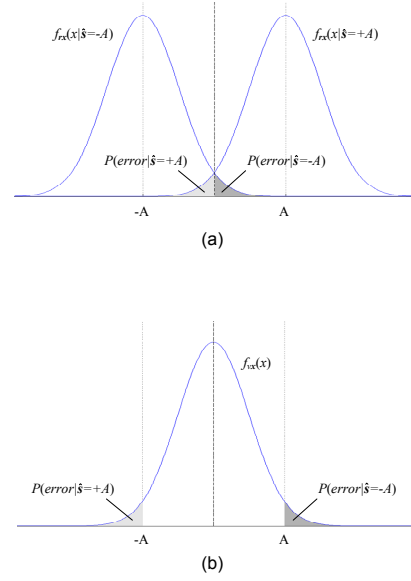


Fig. 2: Error probability for binary signaling.

font denotes a RV. \mathcal{P}_e is computed from the theorem of total probability

$$\mathcal{P}_e = \mathcal{P}\{\mathbf{r}_x > 0 | \hat{\mathbf{s}} = -A\} \mathcal{P}\{\hat{\mathbf{s}} = -A\} + \mathcal{P}\{\mathbf{r}_x \leq 0 | \hat{\mathbf{s}} = A\} \mathcal{P}\{\hat{\mathbf{s}} = A\} \quad (3)$$

where Equation (3) is simplified in two ways. First, it is assumed that binary 0 and 1 are equally probable, i.e., $\mathcal{P}\{\hat{\mathbf{s}} = \pm A\} = \frac{1}{2}$. Second, understanding that \mathbf{r}_x , given that $\hat{\mathbf{s}} = \pm A$, are just shifted versions of \mathbf{v}_x (as illustrated in Figure 2) allows for the conditional probabilities to be written as

$$\mathcal{P}\{\mathbf{r}_x > 0 | \hat{\mathbf{s}} = -A\} = \mathcal{P}\{\mathbf{v}_x > A\} \quad (4)$$

$$\mathcal{P}\{\mathbf{r}_x \leq 0 | \hat{\mathbf{s}} = A\} = \mathcal{P}\{\mathbf{v}_x \leq -A\} \quad (5)$$

Substitution and expressing the probabilities in integral form gives

$$\mathcal{P}_e = \frac{1}{2} \mathcal{P}\{\mathbf{v}_x > A\} + \frac{1}{2} \mathcal{P}\{\mathbf{v}_x \leq -A\} \quad (6)$$

$$= \frac{1}{2} \int_A^{\infty} f_{\mathbf{v}_x}(x) dx + \frac{1}{2} \int_{-\infty}^{-A} f_{\mathbf{v}_x}(x) dx \quad (7)$$

where $f_{\mathbf{v}_x}(x)$ is the probability distribution function (PDF) of \mathbf{v}_x .

Probability of a bit error is determined by evaluating the integrals in equation (7), as illustrated in Figure 2(b). Theoretical results are derived from analytic solutions, and quasi-analytic results are approximated by generating sample functions of the appropriate random processes. In the following subsections, theoretical results are presented for receiver CGN (i.e., no undesired signal), undesired CGN + receiver CGN, and undesired constant + receiver CGN.

3.1. Receiver CGN

Without the influence of an undesired signal, $\hat{\mathbf{v}}$ is zero-mean CGN. The real part is Gaussian distributed with zero mean and variance σ_n^2 , which is commonly abbreviated as $\mathbf{v}_x = \mathbf{N}[0, \sigma_n^2]$. The PDF of \mathbf{v}_x is

$$f_{\mathbf{v}_x}(x) = \frac{1}{\sqrt{2\pi}\sigma_n} \exp\left[-\frac{x^2}{2\sigma_n^2}\right]. \quad (8)$$

Substitution into equation (7) and change of variables allows for the integrals to be combined to give

$$\mathcal{P}_e = \int_{A/\sigma_n}^{\infty} \frac{1}{\sqrt{2\pi}} e^{-\lambda^2/2} d\lambda = Q\left(\frac{A}{\sigma_n}\right), \quad (9)$$

where $Q(\xi) = \int_{\xi}^{\infty} e^{-\lambda^2/2} d\lambda = \frac{1}{2} \operatorname{erfc}\left(\frac{\xi}{\sqrt{2}}\right)$ is the cumulative distribution function of the standard normal deviate.

It is useful to express error probability in terms of mean signal powers, i.e.,

$$\mathcal{P}_e = Q\left(\sqrt{2\frac{P_s}{P_n}}\right), \quad (10)$$

where $P_s = \mathcal{E}\{|\hat{s}|^2\} = A^2$, and $P_n = 2\sigma_n^2$ is determined by b and the power density of the receiver noise.

Figure 3 illustrates \mathcal{P}_e versus P_s/P_n . Notice that $\mathcal{P}_e(P_s/P_n = 8.4 \text{ dB}) \approx 10^{-4}$. As stated previously, this defines the operational scenario of the BPSK receiver onto which the undesired signals are imposed.

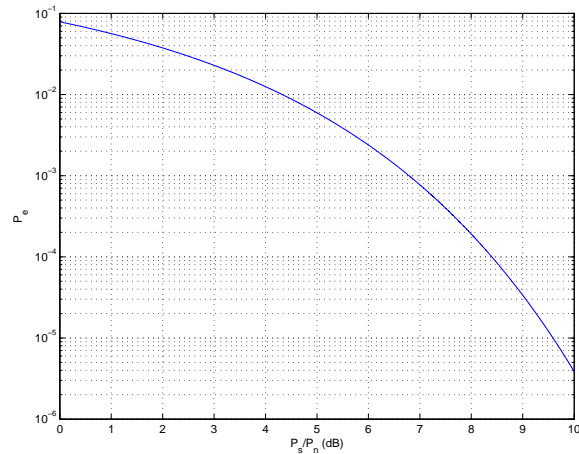


Fig. 3: Theoretical error probability vs. signal-to-noise ratio for a BPSK receiver operating in CGN.

3.2. Undesired CGN + Receiver CGN

Undesired CGN is the reference to which other undesired signals are compared in this study. Undesired Gaussian noise at the radio frequency is CGN at CBB

with a zero-mean Gaussian real part. As stated previously, receiver noise is also CGN. The sum of two independent Gaussian RVs is a Gaussian RV with a mean and variance equal to the sum of the means and variances. Hence, the PDF of $\hat{\mathbf{v}}_x = \mathbf{N}[0, \sigma_u^2 + \sigma_n^2]$ is

$$f_{\hat{\mathbf{v}}_x}(x) = \frac{1}{\sqrt{2\pi(\sigma_u^2 + \sigma_n^2)}} \exp\left[-\frac{x^2}{2(\sigma_u^2 + \sigma_n^2)}\right]. \quad (11)$$

Substitution into equation (7) gives error probability as

$$\mathcal{P}_e = Q\left(\frac{A}{\sqrt{\sigma_n^2 + \sigma_u^2}}\right) = Q\left(\sqrt{\frac{2\frac{P_s}{P_n}}{1 + \frac{P_u}{P_n}}}\right). \quad (12)$$

In this expression, average power of the undesired signal, $P_u = 2\sigma_u^2$, is determined by b and power density of the undesired CGN. Average power of the receiver noise, P_n is established by the specified signal-to-noise ratio. Equation (12) is a reference curve plotted in \mathcal{P}_e versus P_u/P_n graphs to compare other undesired signals to undesired CGN.

3.3. Undesired Constant + Receiver CGN

Undesired CW (assumed to be centered within the bandwidth of the victim receiver) at CBB is a constant with a real part equal to $v_c \cos \theta_c$, where v_c is the constant voltage and θ_c is the offset angle. Adding this constant only alters the mean of the resulting undesired-plus-noise signal, i.e., $\mathbf{v}_x = \mathbf{N}[v_c \cos \theta_c, \sigma_n^2]$, and the PDF is given by

$$f_{\mathbf{v}_x}(x) = \frac{1}{\sqrt{2\pi}\sigma_n} \exp\left[-\frac{(x - v_c \cos \theta_c)^2}{2\sigma_n^2}\right]. \quad (13)$$

Substitution into equation (7) and change of variable gives error probability as

$$\begin{aligned} \mathcal{P}_e &= \frac{1}{2} \sum_{k=0}^1 Q\left(\frac{A - (-1)^k v_c \cos \theta_c}{\sigma_n}\right) \\ &= \frac{1}{2} \sum_{k=0}^1 Q\left(\sqrt{2\frac{P_s}{P_n}} - (-1)^k \sqrt{2\frac{P_u}{P_n} \cos^2 \theta_c}\right), \end{aligned} \quad (14)$$

$$(15)$$

where $P_u/P_n = \frac{v_c^2}{2\sigma_n^2}$.

Figure 4 illustrates \mathcal{P}_e versus P_u/P_n for a BPSK receiver exposed to undesired constant with different phase offset angles, $\theta_c = \{0^\circ, 30^\circ, 45^\circ, 60^\circ, 90^\circ\}$. Notice that \mathcal{P}_e is dependent on θ_c , and more importantly that $\theta_c = 0$ degrees causes the highest error probability.

Figure 5 illustrates APDs for a variety of Nakagami-Rice distributions corresponding to different constant levels. Amplitudes of a constant plus CGN are independent of phase and described with the Nakagami-Rice PDF

$$f_{\mathbf{w}}(w) = \frac{1}{w_s} e^{-(w+w_c)/w_s} I_0\left(\frac{2\sqrt{w_c w}}{w_s}\right), \quad (16)$$

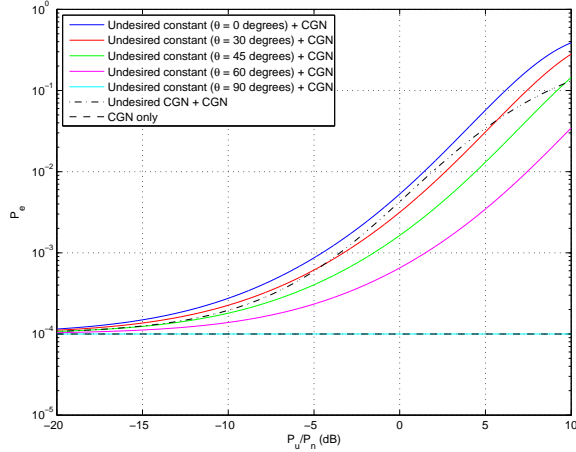


Fig. 4: Theoretical error probability versus P_u/P_n for a BPSK receiver operating at $P_s/P_n \approx 8.4$ dB and exposed to an undesired constant signal.

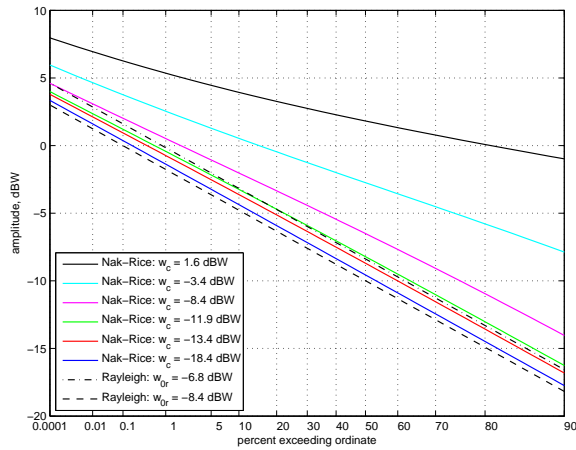


Fig. 5: Nakagami-Rice APDs of constant plus CGN ($w_s = -8.4$ dBW).

where $w_s = 2\sigma_n^2$ is the scattered power, $w_c = v_c^2$ is the constant power, and I_0 is a zero-order modified Bessel function. Equation (16) was integrated numerically with the Quadrature-Romberg algorithm to obtain the APD at a desired accuracy. Also illustrated are Rayleigh-distributed amplitudes of CGN with an APD defined as

$$\mathcal{P}\{\mathbf{w} > w\} = e^{-w/w_{0r}} \quad (17)$$

where $w_{0r} = \mathcal{E}\{\mathbf{w}\}$ is mean power and $\mathbf{w} = |\mathbf{v}|^2$ is normalized instantaneous power dissipated in a $1 - \Omega$ resistor. The APD of CGN is a straight-line on Rayleigh graph paper with w_{0r} corresponding to the 37th percentile. The two Rayleigh APDs in this figure describe noise amplitudes that produce $\mathcal{P}_e = 10^{-3}$ and $\mathcal{P}_e = 10^{-4}$ for a received BPSK signal with $\hat{s} = \pm 1$.

4. SAMPLE FUNCTION ANALYSES

Unfortunately, $f_{\mathbf{v}_x}$ is often too complicated to integrate analytically, especially when considering the effects of band-limiting by the victim receiver. When analytic solutions of equation (7) are unavailable, a quasi-analytic approximation is used. In this approach, a sample function of the undesired signal plus receiver noise, i.e.,

$$\hat{v}_k = \hat{u}_k * \hat{h}_{R,k} + \hat{n}_k \quad (18)$$

is used to represent realizations of the corresponding random process.

A CGN sample function can be generated with

$$\hat{n}_k = z_k e^{j\theta_k} \quad (19)$$

where z_k is a Rayleigh-distributed sample function, and θ_k is a uniformly-distributed sample function with values between 0 and 2π . The inverse method [3] is employed to generate less-common deviates from well-known distributions. From equation (17), for example, Rayleigh amplitudes can be generated by

$$z_k = \sqrt{w_{0r}} [-\ln(\psi_k)]^{1/2} \quad (20)$$

where ψ_k is uniformly-distributed between 0 and 1.

Probabilities in equation (6) are approximated with

$$\mathcal{P}\{\mathbf{v}_x > A\} \approx \frac{\ell_+}{L} \quad \text{and} \quad \mathcal{P}\{\mathbf{v}_x \leq -A\} \approx \frac{\ell_-}{L} \quad (21)$$

where ℓ_+ is the number of samples in $\text{Re}[\hat{v}_k]$ that exceed $+A$, ℓ_- is the number of samples in $\text{Re}[\hat{v}_k]$ less than or equal to $-A$, and L is the total number of samples in \hat{v}_k . Note that \mathcal{P}_e results given in this section were approximated with sample functions of $L = 10^7$, and APDs were calculated with 10^6 samples.

In the following subsections, expressions for generating \hat{u}_k are given for substitution into equation (18). Subsequent quasi-analytic approximations to \mathcal{P}_e versus P_u/P_n for a BPSK receiver exposed to MPSK + CGN, impulsive noise + CGN, and gated CGN + CGN are also provided. Note that it is necessary to calculate P_u explicitly from the sample function generated by $\hat{h}_{R,k} * \hat{u}_k$ because it depends on the power spectral density of the undesired signal in addition to the bandwidth of the BPSK victim receiver.

4.1. Undesired MPSK + Receiver CGN

MPSK signals are phase-modulated pulses passed through a transmit filter. Modulation is specified by the number of symbols (M), e.g., $M = 2$ for BPSK, and offset angle (θ_u), which orients the constellation in the complex plane. An MPSK sample function can be generated with

$$\hat{u}_k = \hat{h}_{T,k} * A_u \exp \left[j \left(\frac{2\pi m_k}{M} + \theta_u \right) \right] \quad (22)$$

where m_k are uniformly-distributed integers ranging from 0 to $M - 1$, and $\hat{h}_{T,k}$ is the impulse response of the RRC transmit filter.

Figure 6 gives performance curves for a BPSK receiver exposed to a BPSK interfering signal with $b_u = 1$ MHz, $a_u = 0.35$, and $\theta_u = \{0^\circ, 45^\circ\}$. Figure 7 illustrates APDs of sample functions for BPSK signals ($\theta_u = 0^\circ$) at a variety of mean powers.

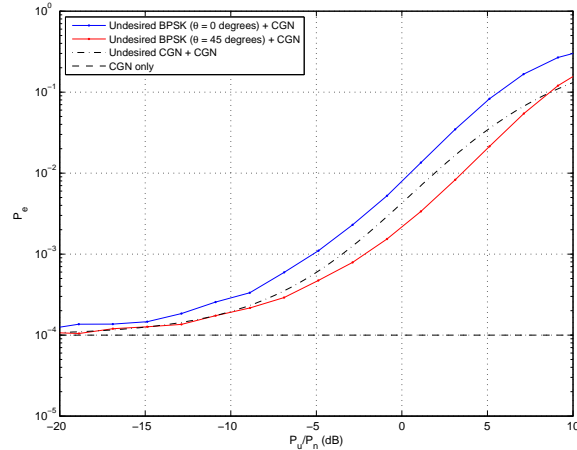


Fig. 6: Error probability versus P_u/P_n for a BPSK receiver ($b = 1$ MHz, $a = 0.35$) operating at $P_s/P_n \approx 8.4$ dB and exposed to undesired BPSK ($b_u = 1$ MHz, $a_u = 0.35$).

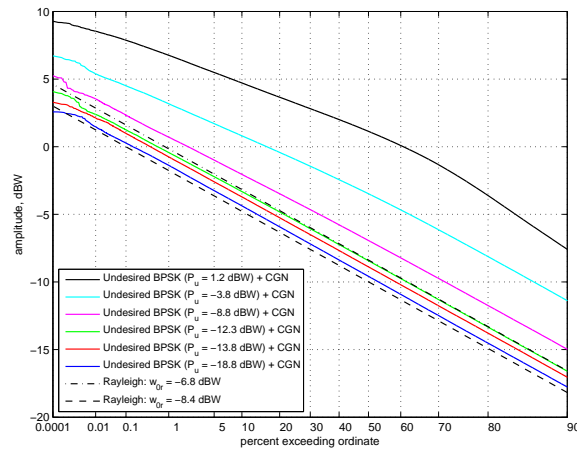


Fig. 7: APDs of undesired BPSK ($b_u = 1$ MHz, $a_u = 0.35$) plus CGN ($P_n = -8.4$ dBW) after the receiver filter ($b = 1$ MHz, $a = 0.35$).

4.2. Undesired Impulsive Noise + Receiver CGN

Impulsive noise can be due to unintentional man-made radiation, such as power lines and automotive ignition systems, or natural sources, such as lightning. The impulsive noise model described in this subsection was

developed and utilized in [4] to reduce measured man-made noise data to a meaningful set of noise parameters and consequently provide a straight-forward means for evaluating receiver performance.

Assuming uniform phase, a sample function of impulsive noise can be written as

$$\hat{u}_k = z_k^{(\alpha)} \chi_k e^{j\theta_k} \quad (23)$$

where $z_k^{(\alpha)}$ is a Weibull-distributed sample function, and χ_k is a binary sample function that determines the presence of a pulse.

Weibull amplitudes are described by the APD

$$\mathcal{P}\{\mathbf{w} > w\} = \exp\left[-\frac{w}{w_{0w}}\right]^{1/\alpha} \quad (24)$$

where w_{0w} and α are Weibull parameters. The inverse method permits generation of a Weibull-distributed sample function via

$$z_k^{(\alpha)} = \sqrt{w_{0r}} [-\ln(\psi_k)]^{\alpha/2} \quad (25)$$

Mean power of a RV with Weibull amplitudes is $\mathcal{E}\{\mathbf{w}\} = w_{0w} \Gamma(\alpha + 1)$. Note that the Weibull APD reduces to equation (17) when $\alpha = 1$.

Pulse time of arrival is assumed to be Poisson distributed with pulse arrival rate γ . The probability that one pulse will arrive in Δt seconds is $\gamma \Delta t$; therefore, the presence of a pulse is determined by

$$\chi_k = \begin{cases} 1 & \text{if } \psi_k \leq \gamma \Delta t \\ 0 & \text{otherwise} \end{cases} \quad (26)$$

Figure 8 gives performance curves for a BPSK receiver exposed to impulsive noise with $\alpha = 4$ and $\gamma = \{10^2, 10^3, 10^4, 10^5\}$ pulses per second. Figure 9 illustrates APDs of sample functions for impulsive noise ($\gamma = 10^3$ pulses/s, $\alpha = 4$) at various mean powers. Notice the high variability in mean undesired power when pulse events are rare.

4.3. Undesired Gated Noise + Receiver CGN

Undesired gated noise is a cyclo-stationary process used to emulate certain types of UWB signals that periodically turn on and off or hop in and out of the operational band of a victim receiver. To describe the amplitude and time statistics of undesired gated noise, a statistical model developed in [5] is employed. The model is written as

$$\hat{u}_k = z_k^{(\alpha)} g_k(T_g, \tau_{on}) e^{j\theta_k} \quad (27)$$

where $z_k^{(\alpha)}$ is a Weibull-distributed sample function that can be generated with equation (25). The gating function is defined as

$$g_k(T_g, \tau_{on}) = \sum_{q=-\infty}^{\infty} R(k\Delta t - qT_g; T_g, \tau_{on}) \quad (28)$$

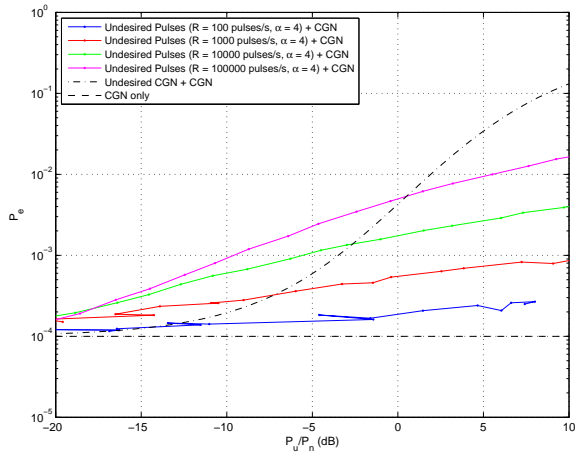


Fig. 8: Error probability versus P_u/P_n for a BPSK receiver ($b = 1$ MHz, $a = 0.35$) operating at $P_s/P_n \approx 8.4$ dB and exposed to undesired impulsive noise.

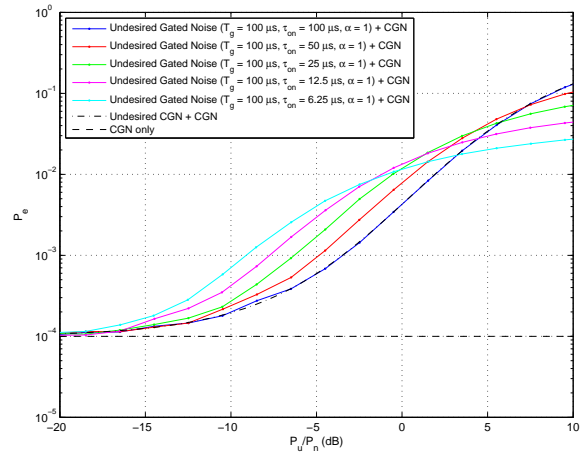


Fig. 10: Error probability versus P_u/P_n for a BPSK receiver ($b = 1$ MHz, $a = 0.35$) operating at $P_s/P_n \approx 8.4$ dB and exposed to undesired gated noise.

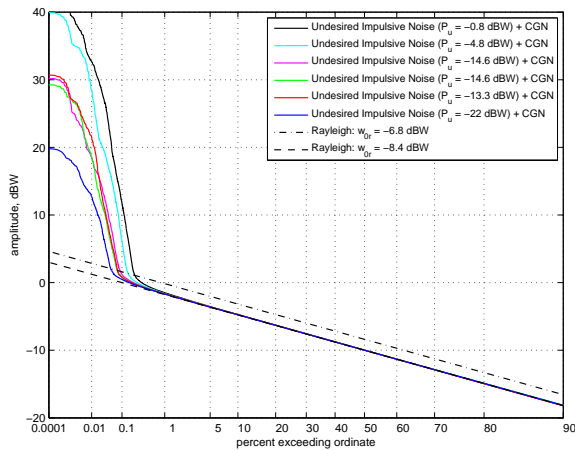


Fig. 9: APDs of undesired impulsive noise ($\gamma = 10^3$ pulses/s, $\alpha = 4$) plus CGN ($P_n = -8.4$ dBW) after the receiver filter ($b = 1$ MHz, $a = 0.35$).

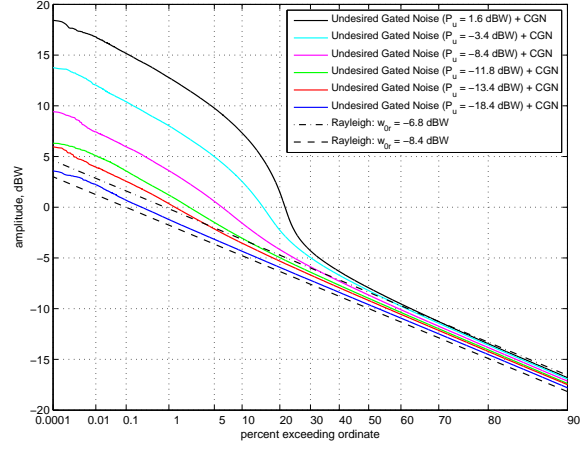


Fig. 11: APDs of undesired gated noise ($T_g = 100$ μ s, $\tau_{on} = 25$ μ s, $\alpha = 1$) plus CGN ($P_n = -8.4$ dBW) after the receiver filter ($b = 1$ MHz, $a = 0.35$).

where

$$R(t; T_g, \tau_{on}) = \begin{cases} 1 & \text{if } 0 \leq t < \tau_{on} \\ 0 & \text{if } \tau_{on} \leq t < T_g \end{cases}, \quad (29)$$

τ_{on} is the gate on-time, T_g is the gate period, and q is an integer.

Figure 10 gives performance curves for a BPSK receiver exposed to undesired gated-noise with $T_g = 100$ μ s, $\tau_{on} = \{100, 50, 25, 12.5, 6.25\}$ μ s, and $\alpha = 1$. Figure 11 illustrates APDs of sample functions for gated-noise ($T_g = 100$ μ s, $\tau_{on} = 25$ μ s, $\alpha = 1$) at various mean powers.

5. DISCUSSION

This paper describes a methodology for assessing demodulator performance in the presence of various types of undesired signals. The goal is to help spectrum engineers understand how different undesired signals affect a victim digital receiver in order to develop fair spectrum policy.

One application is to assess the interference effects of new spectrum sharing technologies. This is done by comparing \mathcal{P}_e of an undesired signal to equal power of CGN. For the cases illustrated in this paper, undesired constant signals were generally less detrimental to BPSK demodulator performance than CGN. Undesired BPSK

appeared more-or-less “noise-like.” Impulsive noise with relatively low pulse rate was less detrimental than CGN, but its impact increased with higher pulse rates. Finally, both impulsive noise and gated noise were less detrimental than undesired CGN at relatively high P_u/P_n .

A second application is to validate receiver susceptibility measurements. Figure 12 compares \mathcal{P}_e predictions to susceptibility measurements of a digital television (DTV) receiver exposed to undesired gated Gaussian noise [5]. The tested DTV system utilized quadrature phase-shift keying (QPSK) with a RRC matched filter ($a = 0.35$) and a symbol rate of 19.51 Mbaud. The DTV receiver, operating at $P_s/P_n \approx 11$ dB, was exposed to gated Gaussian noise with on-time $\tau_{on} = 100 \mu s$ and gating periods $T_g = \{100, 200, 400, 800, 1600\} \mu s$. QPSK modulation is the superposition of two orthogonal BPSK modulations. Hence, QPSK \mathcal{P}_e predictions are identical to BPSK \mathcal{P}_e except for a 3-dB horizontal shift. Good agreement is demonstrated between quasi-analytic predictions and measurements.

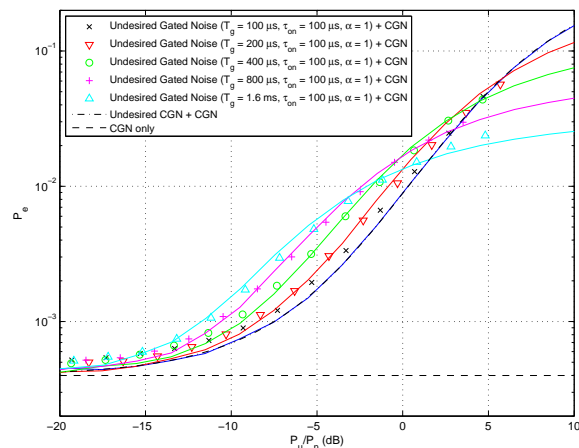


Fig. 12: Comparison between sample-function predictions (lines) and measured DTV susceptibility measurements (data points). QPSK receiver operated at $P_s/P_n \approx 11$ dB and was exposed to undesired gated-noise ($\tau_{on} = 100 \mu s$).

There are a number of areas where we intend to extend this work. An uncertainty analysis will be performed to achieve confidence intervals for the quasi-analytic results. This uncertainty is a function of L and can be observed in quasi-analytic \mathcal{P}_e results at low undesired power levels and sample-function APDs at low percentiles. The methodology will also be extended to other interferers, e.g., bursty noise, aggregate sources, radar pulses, orthogonal frequency-division multiplexing signals, and other types of noise. Finally, correlations between \mathcal{P}_e and statistical characteristics of \hat{v} (e.g., APD [2], level crossing statistics) will be further analyzed.

ACKNOWLEDGMENT

The author would like to thank Robert Achatz, Dr. Roger Dalke, and Dr. George Hufford for sharing knowledge and enthusiasm on the subject. A special thanks is extended to Dr. Hufford for sharing his insight in statistical distributions, which has been central to my understanding on the subject.

REFERENCES

- [1] Department of Commerce, “Spectrum management for the 21st century: Plan to implement recommendations of the President’s Spectrum Policy Initiative,” Mar. 2006.
- [2] K. Wiklundh, “Relation between the amplitude probability distribution of an interfering signal and its impact on digital radio receivers,” *IEEE Transactions on Electromagnetic Compatibility*, Vol. 48, No. 3, pp. 537–544, Aug. 2006.
- [3] M. Abramowitz and I.A. Stegun, *Handbook of mathematical functions*, NBS Applied Math Series 55, New York, NY: Dover Publishing, 1964.
- [4] R.J. Achatz, Y. Lo, P.B. Papazian, R.A. Dalke, and G.A. Hufford, “Man-made noise in the 136 to 138-MHz VHF meteorological satellite band,” NTIA Report 98-355, Sep. 1998.
- [5] M. Cotton, R. Achatz, J. Wepman, and P. Runkle, “Interference potential of ultrawideband signals: Part 2 - Measurement of gated-noise interference to C-band satellite digital television receivers,” NTIA Report TR-05-429, Aug. 2005.